Supplement 1

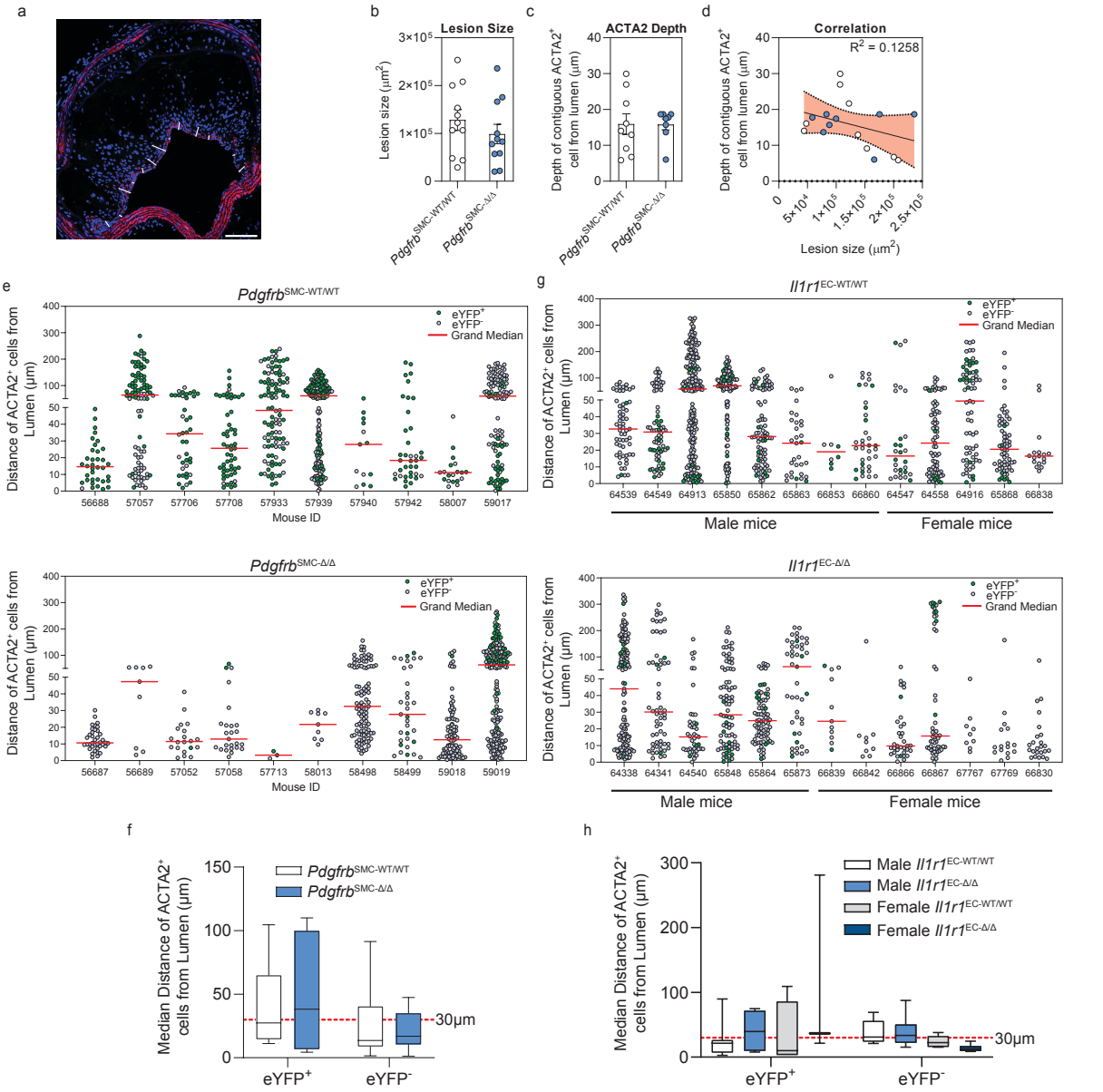

Supplement 1: Analysis of contiguous ACTA2⁺ cell area depth and sub-luminal depth of all ACTA2⁺ cells. (A) Representative image showing assessment of contiguous fibrous cap depth based on ACTA2 staining. **(B)** Area of lesions from from *Pdgfrb*$^{SMC\text{-}WT/WT}$ and *Pdgfrb*$^{SMC\text{-}\Delta/\Delta}$ mice fed 18 weeks of WD. **(C)** Distance from lumen to average distal point of contiguous ACTA2⁺ area, determined by drawing a perimeter encompassing ACTA2⁺ cells, maintaining a continuous layer. **(D)** Correlation analysis between ACTA2⁺ cell depth and lesion size using a linear regression. Statistical analysis was performed with a t-test with Welch's correction. Error bands represent (5% confidence interval. **(E)** Distance of each ACTA2⁺ cell from the lumen of individual *Pdgfrb*$^{SMC\text{-}WT/WT}$ or *Pdgfrb*$^{SMC\text{-}\Delta/\Delta}$ mice, distinguishing between *Myh11*-eYFP⁺ and *Myh11*-eYFP⁻ cells. **(F)** Quantification of the median distance of ACTA2⁺ cells from the lumen across all sample groups in **(E)** **[**eYFP⁺ WT – Min: 11.26; 25%: 14.56; Med: 27.46; 75%: 64.84; Max: 104.6**],** **[**eYFP⁺ KO – Min: 4.417; 25%: 6.821; Med: 38.14; 75%: 99.86; Max: 110.1**],** **[**eYFP⁻ WT – Min: 1.533; 25%: 8.740; Med: 13.62; 75%: 40.39; Max: 91.44**],** **[**eYFP⁻ KO – Min:1.241; 25%: 10.51; Med: 16.92; 75%: 35.10; Max: 47.36**]**.. **(G)** Distance of each ACTA2⁺

cell from the lumen of individual *Il1r1*$^{EC\text{-}WT/WT}$ and *Il1r1*$^{EC\text{-}\Delta/\Delta}$ mice, separated by sex. **(H)** Quantification of the median distance of ACTA2^{+} cells from the lumen across all sample groups in **(G) [**eYFP^{+} Male WT – Min: 2.841; 25%: 6.687; Med: 21.55; 75%: 26.41; Max: 89.66**], [**eYFP^{+} Male KO – Min: 7.669; 25%: 9.674; Med: 39.67; 75%: 71.56; Max: 74.77**], [**eYFP^{+} Female WT – Min: 3.249; 25%: 3.316; Med: 10.00; 75%: 85.90; Max: 109.0**], [**eYFP^{+} Female KO – Min: 21.48; 25%: 21.48; Med: 36.79; 75%: 281.1; Max: 281.1**], [**eYFP^{-} Male WT – Min: 21.15; 25%: 23.71; Med: 30.84; 75%: 56.10; Max: 69.19**], [**eYFP^{-} Male KO – Min: 15.53; 25%: 22.15; Med: 33.50; 75%: 50.50; Max: 87.61**], [**eYFP^{-} Female WT – Min: 15.26; 25%: 15.83; Med: 22.37; 75%: 32.45; Max: 38.11**], [**eYFP^{-} Female KO – Min: 5.948; 25%: 8.931; Med: 10.92; 75%: 15.69; Max: 24.59**]**. Scale bar: 100μm. Biologically independent animals are indicated as individual dots in **(B, C, D)**, dots represent individual cells in **(E, G)**.

Supplement 2

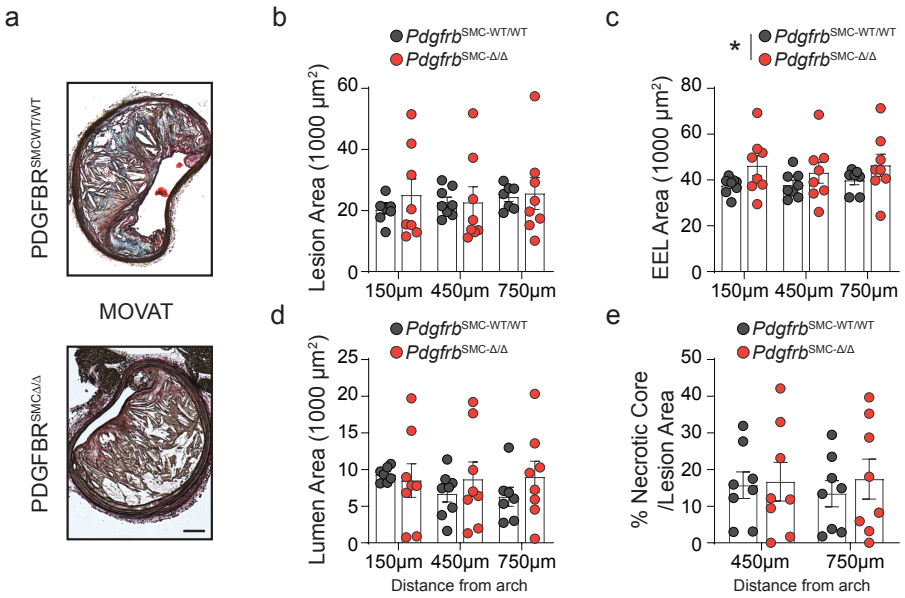

Supplement 2: Lesion morphometry from *Pdgfrb*$^{SMC\text{-}WT/WT}$ and *Pdgfrb*$^{SMC\text{-}\Delta/\Delta}$ mice after 26 weeks of WD feeding. (A) Representative MOVAT images from *Pdgfrb*$^{SMC\text{-}WT/WT}$ and *Pdgfrb*$^{SMC\text{-}\Delta/\Delta}$ mice after 26 weeks of WD. **(B)** Lesion area was not significantly different. **(C)** EEL area was increased across the entire BCA, however lumen area **(D)** was not significantly changed at three locations. **(E)** Necrotic core area was unchanged. Scale bar: 100μm. X-axis values represent distance past the aortic arch. Graphs were analyzed using two-way ANOVA with Sidak correction and multiple comparisons, biologically independent animals are indicated as individual dots, error bars represent mean ± SEM. *p≤0.05.

Supplement 3

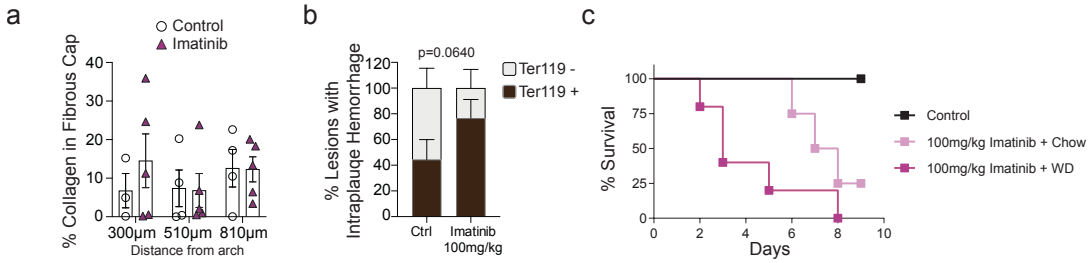

Supplement 3: Collagen content and intraplaque hemorrhage in mice treated with Imatinib. (A) Quantification of collagen content by PicroSirius Red staining and **(B)** intraplaque hemorrhage by Ter119 staining in Imatinib-treated mice. **(C)** Kaplan-Meier survival analysis of mice treated with Imatinib that were fed chow or WD for 18 weeks. X-axis values represent distance past the aortic arch **(A)**. Graphs were analyzed using two-way ANOVA with Sidak correction and multiple comparisons. p-value in **(B)** represents the interaction of treatment and Ter119 status by two-way ANOVA.

Supplement 4

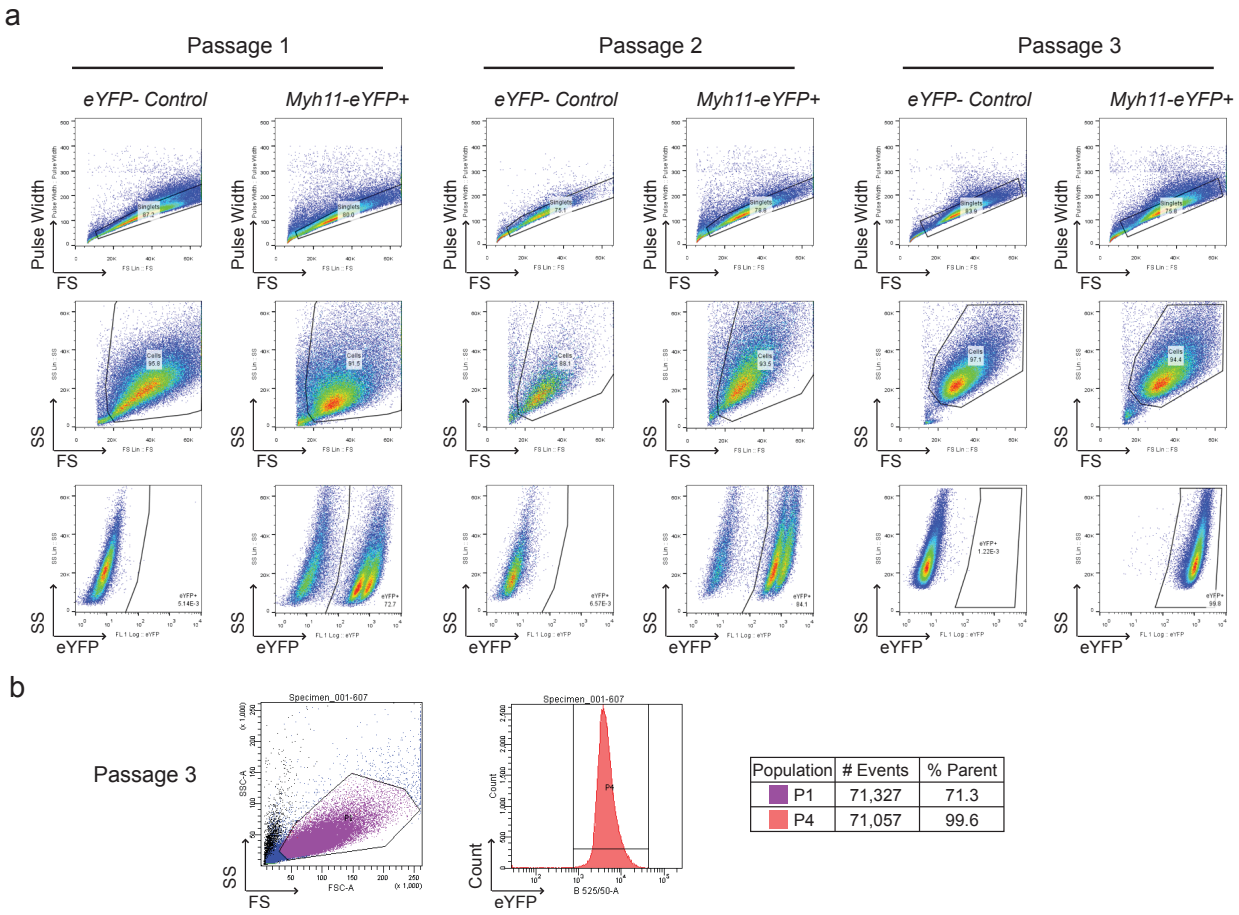

Supplement 4: Isolation of SMC from *Myh11*-CreER^{T2} lineage-tracing mice ensures a pure population of SMC. *Myh11*-CreER^{T2} mice were given tamoxifen prior to SMC isolation to activate *Myh11*-eYFP recombination. **(A)** Vessels were harvested, partially digested to remove adventitia, and then assayed by flow cytometry to determine purity using endogenous eYFP, for three passages. A C57BL/6 mouse line was used as FMO control. **(B)** *Myh11*-eYFP^{+} cells were Flow sorted. *Myh11*-eYFP^{+} cells comprised >99% of the cells after the third passage.

Supplement 5

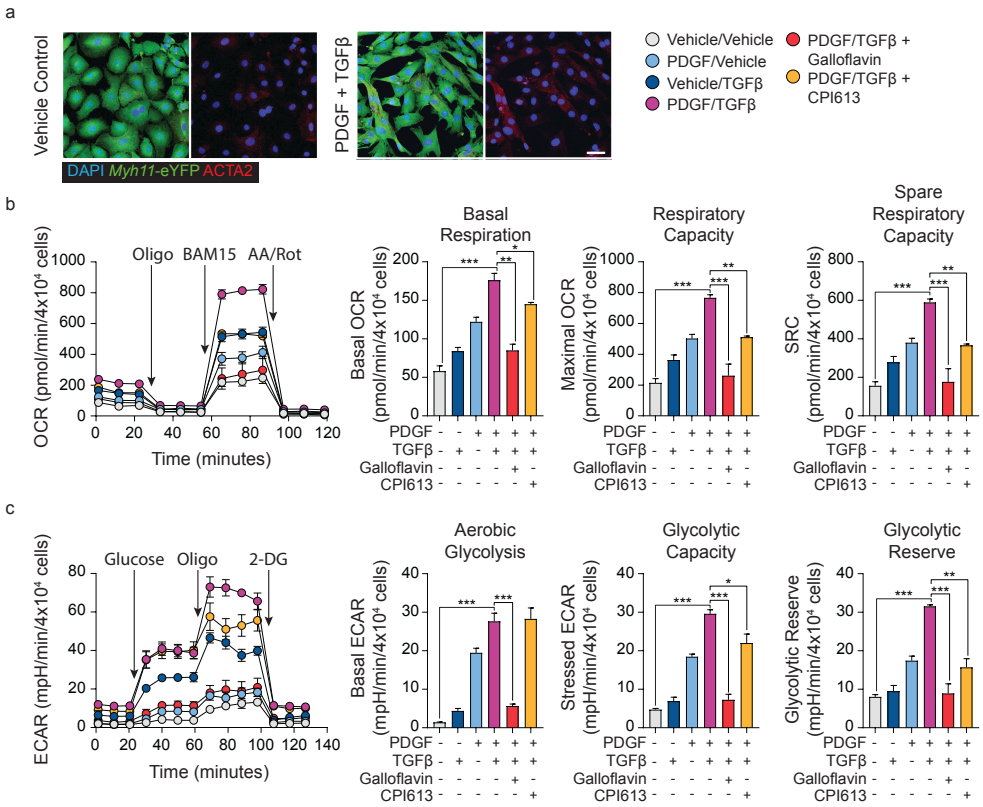

Supplement 5: Morphology and bioenergetics of the SMC-to-myofibroblast transition *in vitro*. Confluent cultured murine aortic SMC were serum starved for 24-72 hours, and then treated with Vehicle (4mM HCl in PBS; DMSO), PDGF-BB (50ng/mL), TGFβ1 (50ng/mL), Galloflavin (10μM), and/or CPI613 (10μM) for an additional 24-48 hours. **(A)** Representative immunofluorescent images. **(B)** Mitochondrial stress test (MST) measuring the oxygen consumption rate (OCR) of cells, representing mitochondrial respiratory ability. OCR was measured initially (basal respiration), and after injection of 1μM oligomycin, 2μM BAM15 (respiratory capacity), and 10μM antimycin A & 1μM rotenone (non-mitochondrial; used for normalization). Spare respiratory capacity was determined by subtracting the initial OCR from the post-BAM15 OCR. **(C)** Glycolytic stress test (GST) measuring extracellular acidification rate (ECAR) of cells, representing glycolytic ability. ECAR was measured initially in the absence of glucose, after injection of 20mM D-glucose (basal glycolysis), 1μM oligomycin (glycolytic capacity), and 80mM 2-deoxy-D-glucose (non-glycolytic; used for normalization). Glycolytic reserve was determined by subtracting post-glucose ECAR from post-oligomycin ECAR. Scale bar: 50μm **(A)**. Graphs were analyzed using one-way ANOVA with Tukey's correction for post-hoc analysis with n ≥ 3, error bars represent mean ± SEM. ***p≤0.001, **p≤0.01, *p≤0.05.

Supplement 6

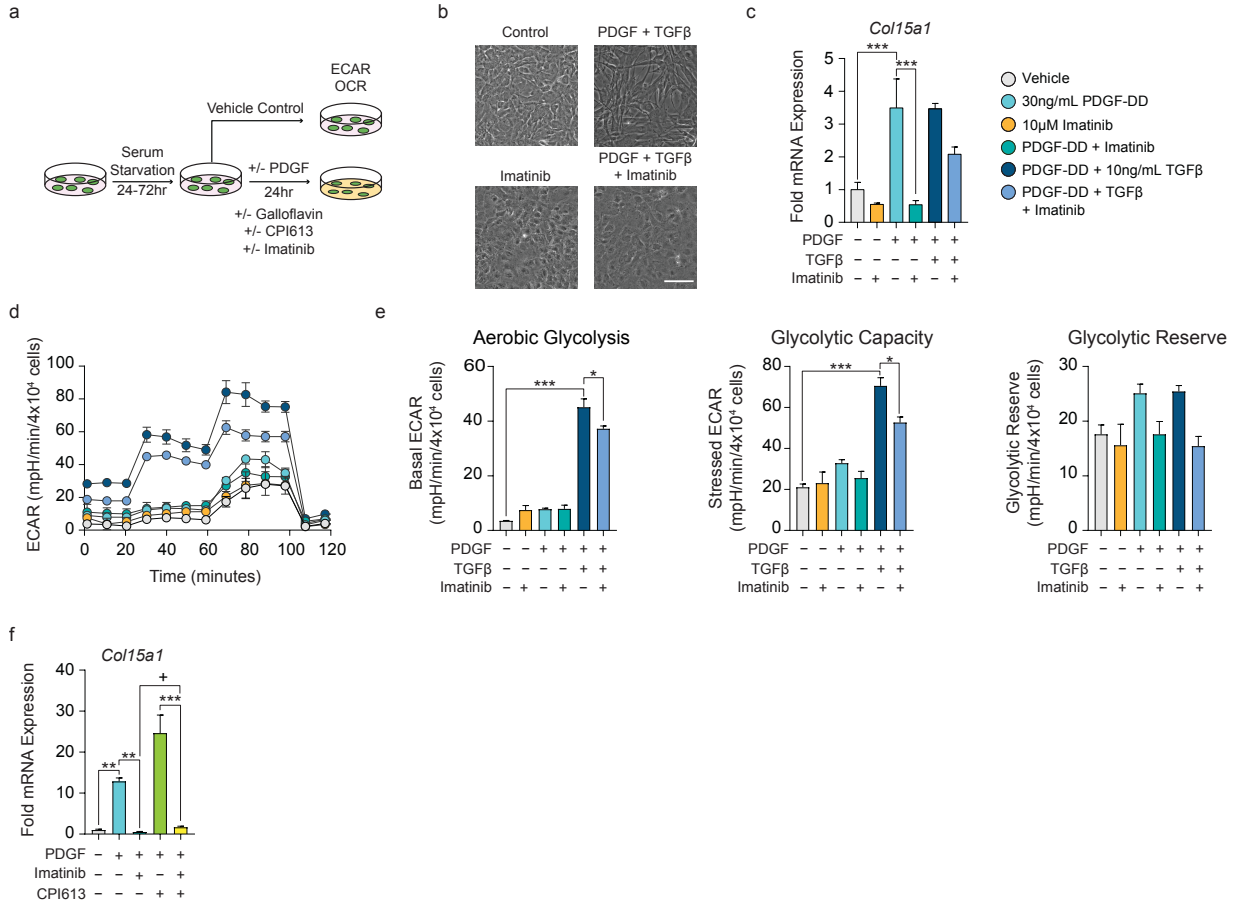

Supplement 6: Imatinib Mesylate induces bioenergetic and transcriptional changes of SMC. (A) Schematic of experimental design. Briefly, murine aortic SMC were serum starved for 24-72 hours. **(B)** Representative phase contrast images taken at 10x magnification. **(C)** mRNA expression of *Col15a1*, measured by qPCR of SMC treated with PDGF-DD (30ng/mL), TGFβ1 (10ng/mL), and/or Imatinib Mesylate (10μM) for 24 hours. **(D)** Glycolytic stress test (GST) measuring extracellular acidification rate (ECAR) representing glycolytic ability of SMC treated with PDGF-DD (30ng/mL), TGFβ1 (10ng/mL), and/or Imatinib Mesylate (10μM) for 24 hours. **(E)** ECAR was measured initially in the absence of glucose, after injection of 20mM D-glucose (basal glycolysis), 1μM oligomycin (glycolytic capacity), and 80mM 2-deoxy-D-glucose (non-glycolytic; used for normalization). Glycolytic reserve was determined by subtracting post-glucose ECAR from post-oligomycin ECAR. **(F)** mRNA expression of *Col15a1*, measured by qPCR in SMC treated with Vehicle, recombinant PDGF-DD (50ng/mL), Imatinib Mesylate (10μM), and/or CPI613 (20μM) for 24 hours. Scale bar: 100μm. Graphs were analyzed using one-way ANOVA with Tukey's correction for post-hoc analysis n≥ 3, error bars represent mean ± SEM. ***p≤0.001, **p≤0.01, *p≤0.05.

Supplement 7

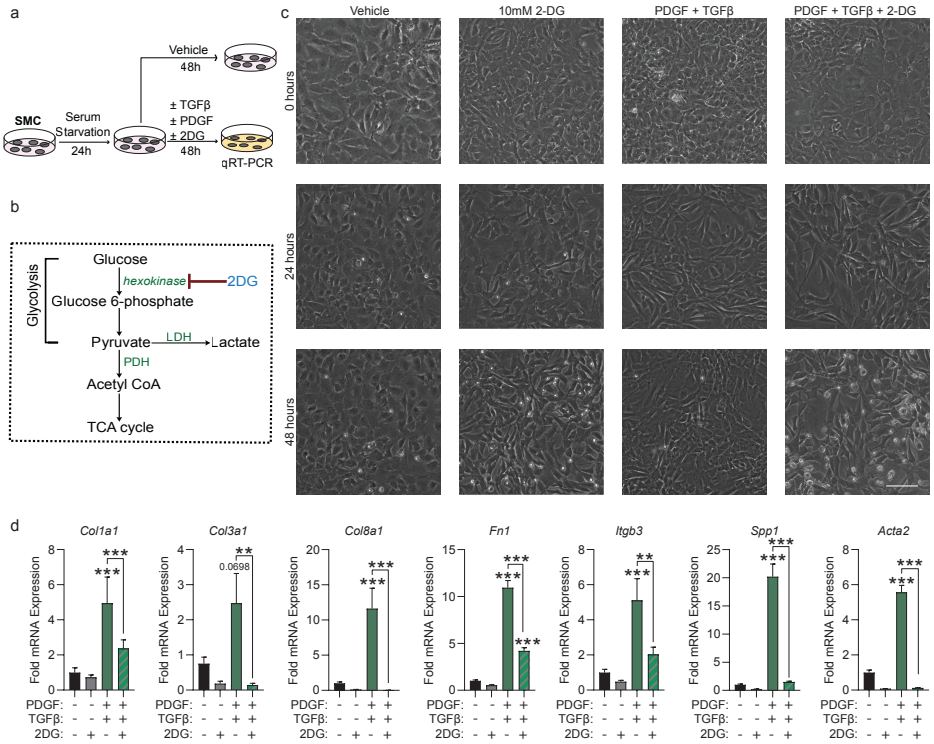

Supplement 7: 2-deoxy-D-glucose (2DG) suppresses expression of PDGF and TGFB-induced genes. (A) Schematic of experimental design. Murine aortic SMC were serum starved for 24-72 hours. After serum starvation, SMCs were treated with vehicle control, PDGF-BB (30ng/mL), TGFβ1 (10ng/mL), and/or 10mM 2-deoxy-D-glucose (2DG; 10mM) for 48 hours. **(B)** Pyruvate metabolism pathway map, highlighting hexokinase as the target of 2-DG. **(C)** Representative phase contrast images taken at 10x magnification taken at timepoints of 0, 24, and 48 hours after treatment. **(D)** mRNA expression of ECM and ECM-interacting genes as measured by qPCR. Scale bar: 100μm. Graphs were analyzed using one-way ANOVA with Tukey's correction for post-hoc analysis with n≥ 3, error bars represent mean ± SEM. ***p≤0.001, **p≤0.01, *p≤0.05.

Supplement 8

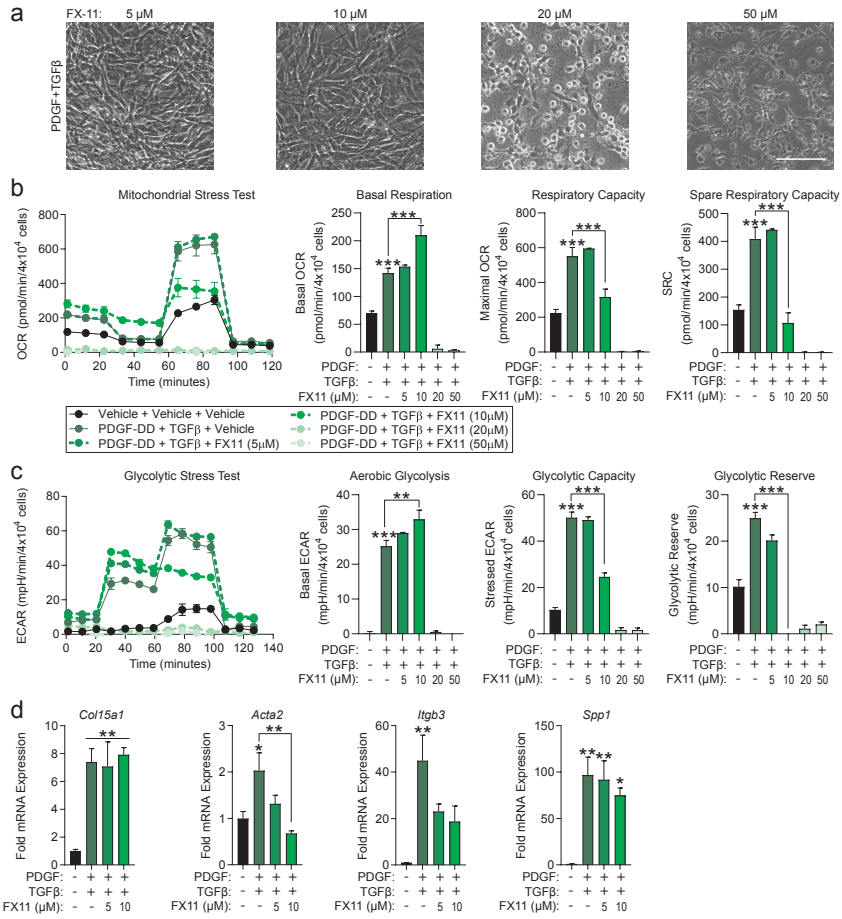

Supplement 8. NADH-competitive inhibitor of aerobic glycolysis, FX-11, has a narrow therapeutic window *in vitro*. Murine aortic SMC were serum starved for 48 hours. After serum starvation, SMCs were treated with vehicle control, PDGF-DD (10ng/mL), TGFβ1 (10ng/mL), and/or LDH inhibitor FX-11 (5-50μM) for 24 hours **(A)** Representative phase contrast images taken at 10x magnification taken after 24 hours of treatment. **(B)** Mitochondrial stress test (MST) measuring the oxygen consumption rate (OCR) of cells, representing mitochondrial respiratory ability. OCR was measured initially (basal respiration), and after injection of 1μM oligomycin, 2μM BAM15 (respiratory capacity), and 10μM antimycin A & 1μM rotenone (non-mitochondrial; used for normalization). Spare respiratory capacity was determined by subtracting the initial OCR from the post-BAM15 OCR. **(C)** Glycolytic stress test (GST) measuring extracellular acidification rate (ECAR) of treated SMC, representing glycolytic ability. ECAR was measured initially in the absence of glucose, after injection of 20mM D-glucose (basal glycolysis), 1μM oligomycin (glycolytic capacity), and 80mM 2-deoxy-D-glucose (non-glycolytic; used for normalization). Glycolytic reserve was determined by subtracting post-glucose ECAR from post-oligomycin ECAR. **(D)** mRNA expression of ECM and ECM-interacting genes as measured by qPCR. Scale bar: 100μm. Graphs were analyzed using one-way ANOVA with Tukey's correction for post-hoc analysis with n≥ 3, error bars represent mean ± SEM. ***p≤0.001, **p≤0.01, *p≤0.05.

Supplement 9

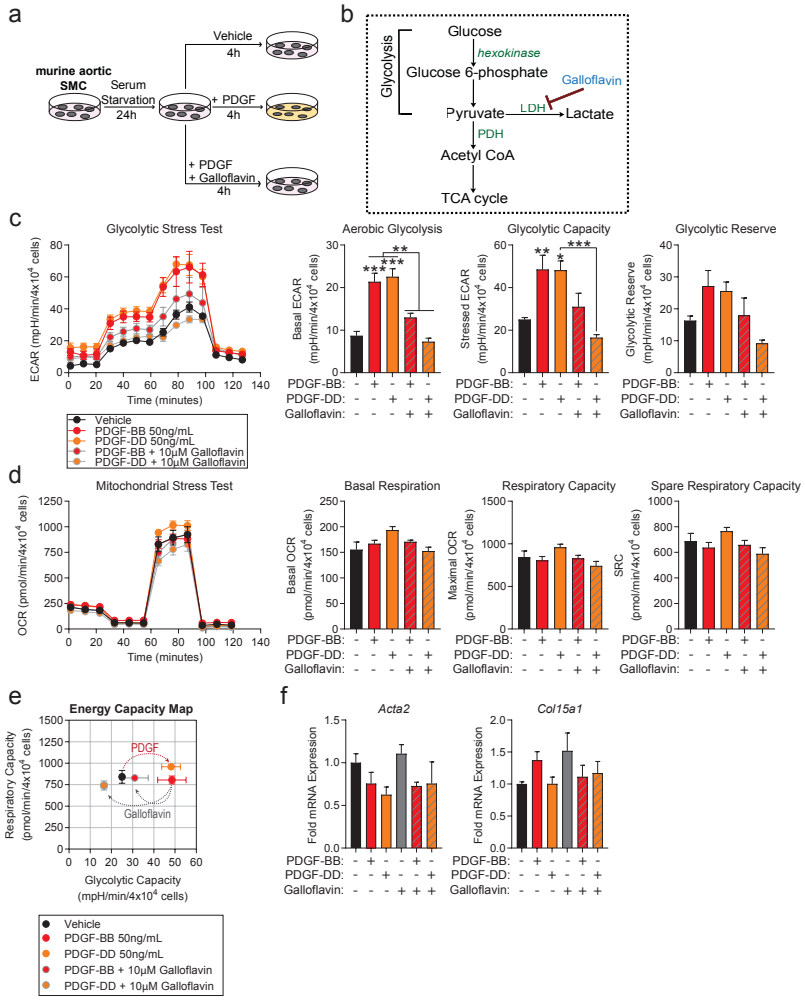

Supplement 9: PDGF drives aerobic glycolysis after 4 hours, prior to induction of respiratory capacity or gene expression. (A) Murine aortic SMC were serum starved for 24-72 hours. After serum starvation, SMCs were treated with vehicle control, PDGF-DD (50ng/mL), PDGF-BB (50ng/mL), and/or LDH inhibitor Galloflavin (10μM) for 24 hours. Schematic showing the abbreviated glycolytic pathway. **(B)** Pyruvate metabolism pathway map, highlighting lactate dehydrogenase (LDH) as the target of Galloflavin. **(C)** Glycolytic stress test (GST) measuring extracellular acidification rate (ECAR) of treated SMC, representing glycolytic ability. ECAR was measured initially in the absence of glucose, after injection of 20mM D-glucose (basal glycolysis), 1μM oligomycin (glycolytic capacity), and 80mM 2-deoxy-D-glucose (non-glycolytic; used for normalization). Glycolytic reserve was determined by subtracting post-glucose ECAR from post-oligomycin ECAR. **(D)** Mitochondrial stress test (MST) measuring the oxygen consumption rate (OCR) of cells, representing mitochondrial respiratory ability. OCR was measured initially (basal respiration), and after injection of 1μM oligomycin, 2μM BAM15 (respiratory capacity), and 10μM antimycin A & 1μM rotenone (non-mitochondrial; used for normalization). Spare respiratory capacity was determined by subtracting the initial OCR from the post-BAM15 OCR. **(E)** Energy capacity map representing the bioenergetic potential of SMC using glycolytic capacity (x-axis, maximal ECAR) and respiratory capacity (y-axis, maximal OCR). **(F)** mRNA expression of *Acta2* and *Col15a1* as measured by qPCR. Graphs were

analyzed using one-way ANOVA with Tukey's correction for post-hoc analysis with n≥ 3, error bars represent mean ± SEM. ***p≤0.001, **p≤0.01, *p≤0.05.

Supplement 10

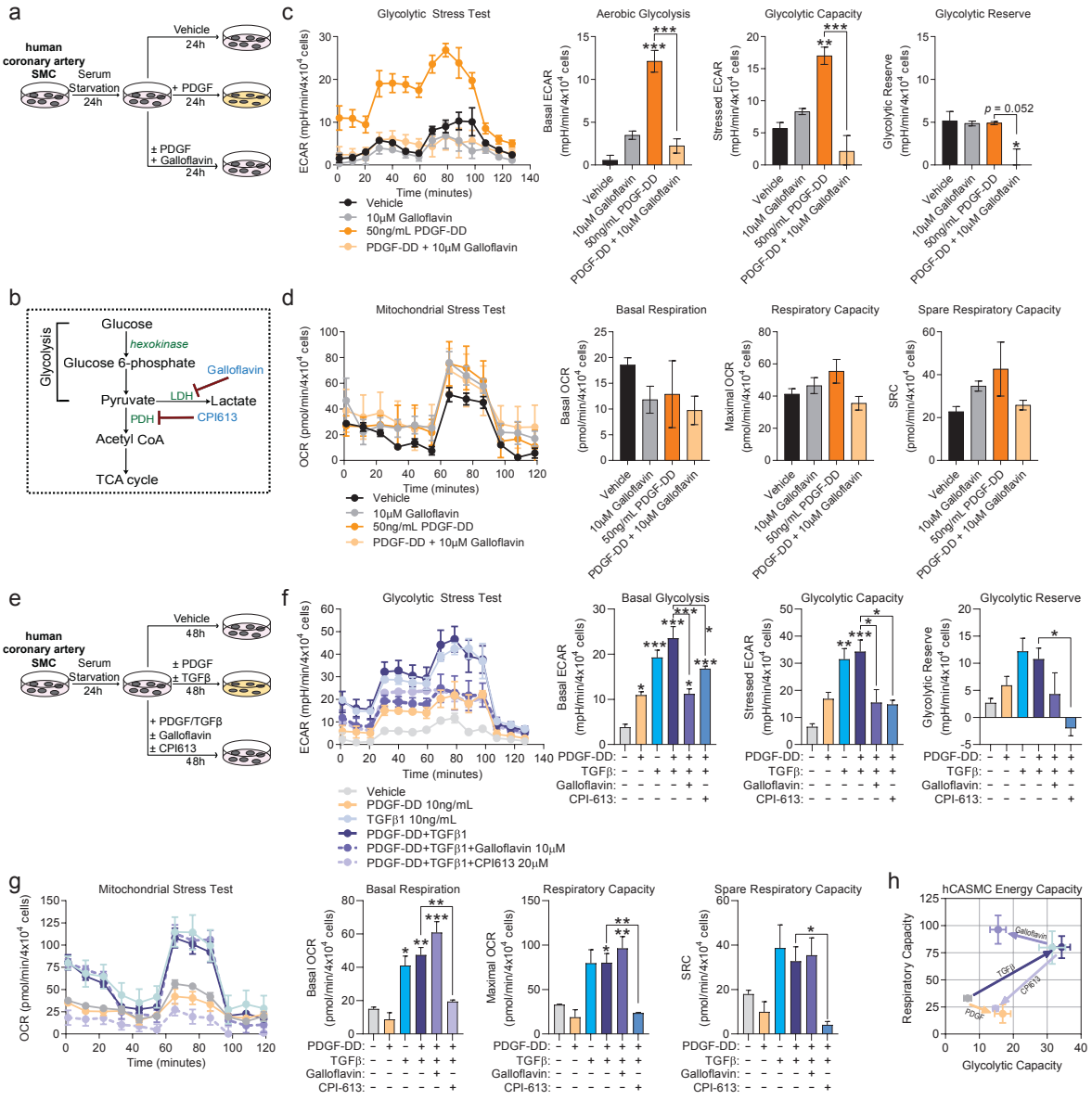

Supplement 10. Human coronary artery SMC (hCASMC) respond to PDGF, TGFβ, Galloflavin, and CPI613 by modulating bioenergetics. (A) Human coronary artery SMC were serum starved for 24-72 hours then treated with vehicle control, PDGF-DD (50ng/mL), and/or Galloflavin (10μM) for 24 hours. **(B)** Pyruvate metabolism pathway map, highlighting lactate dehydrogenase (LDH) as the target of Galloflavin and pyruvate dehydrogenase (PDH) as the target of CPI613. **(C)** Glycolytic stress test (GST) measuring extracellular acidification rate (ECAR) of treated SMC, representing glycolytic ability. ECAR was measured initially in the absence of glucose, after injection of 20mM D-glucose (basal glycolysis), 1μM oligomycin (glycolytic capacity), and 80mM 2-deoxy-D-glucose (non-glycolytic; used for normalization). Glycolytic reserve was determined by subtracting post-glucose ECAR from post-oligomycin ECAR. **(D)** Mitochondrial stress test (MST) measuring the oxygen consumption rate (OCR) of cells, representing mitochondrial respiratory ability. OCR was measured initially (basal respiration), and after injection of 1μM oligomycin, 2μM BAM15 (respiratory capacity), and 10μM antimycin A & 1μM rotenone (non-mitochondrial; used for normalization). Spare respiratory

capacity was determined by subtracting the initial OCR from the post-BAM15 OCR. **(E)** Human coronary artery SMC were serum starved for 24-72 hours then treated with vehicle control, PDGF-DD (10ng/mL) and TGFβ1 (10ng/mL), Galloflavin (10μM), and/or CPI613 (20μM) for 48 hours, with the treatment being refreshed after 24 hours. **(F)** Glycolytic stress test (GST) measuring extracellular acidification rate (ECAR) of treated SMC, representing glycolytic ability. **(G)** Mitochondrial stress test (MST) measuring the oxygen consumption rate (OCR) of cells, representing mitochondrial respiratory ability. **(H)** Energy capacity map representing the bioenergetic potential of SMC using glycolytic capacity (x-axis, maximal ECAR) and respiratory capacity (y-axis, maximal OCR). Graphs were analyzed using one-way ANOVA with Tukey's correction for post-hoc analysis with n≥ 3, error bars represent mean ± SEM. ***p≤0.001, **p≤0.01, *p≤0.05.

Supplement 11

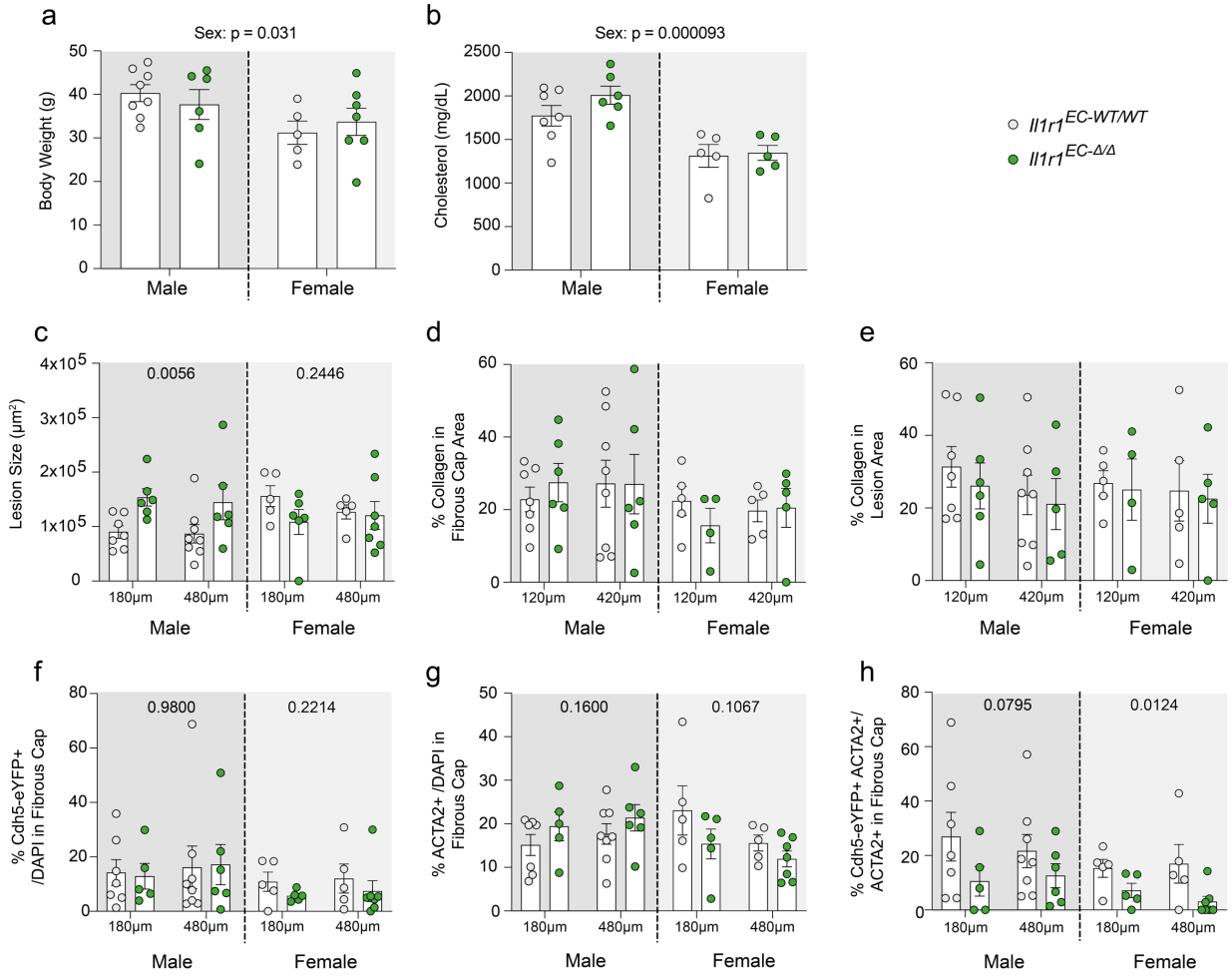

Supplement 11: Analysis for sex-dependent differences in the *Il1r1*$^{EC\text{-}WT/WT}$ and *Il1r1*$^{EC\text{-}\Delta/\Delta}$ mice. There was no difference in body weight **(A)** and cholesterol levels **(B)** were significantly lower in the female mice compared to male mice at the time of harvest. However, there was no difference between genotypes. **(C)** There was a significant increase in lesion size in male mice following knockout of IL1R1 but no effect in the female mice. There was a significant difference in the lesion sizes of the WT mice between sexes (p=0.0035). There was no difference in the collagen content within the fibrous cap **(D)** or the entire lesion area **(E)** between sexes or genotype. **(F)** There was no significant difference in the number of EC that left the lumen monolayer and invested into the fibrous cap and no difference between sexes. **(G)** There was no significant difference in the number of ACTA2^{+} cells in the fibrous cap. **(H)** Both sexes showed a reduction in the contribution of EC to the ACTA2^{+} fibrous cap cells after knockout of IL1R1, however this only achieved statistical significance by two-way ANOVA in the female mice. Graphs were analyzed using two-way ANOVA with Sidak correction and multiple comparisons, biologically independent animals are indicated as individual dots, error bars represent mean ± SEM. p-values displayed in **(C-H)** refer to two-way ANOVA between genotype for each sex.

Supplement 12

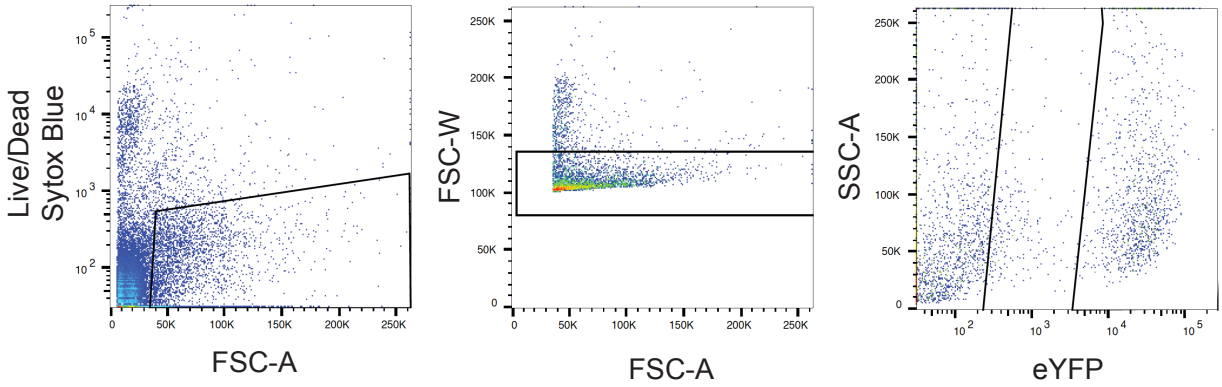

Supplement 12: Gating strategy for scRNAseq datasets. For analysis of medial SMC from PDGFBR WT and KO mice with atherosclerosis, the following gating strategy was employed on single cell preparations: FS vs. Live/dead, FSC-A vs. FSC-W for singlets discrimination, and eYFP vs. SSC-A to identify $eYFP^{+}$ and $eYFP^{-}$ cells.